The Influence of Plasma Membrane Electrostatic Properties on the Stability of Cell Ionic Composition

Stéphane Genet,* Robert Costalat,* and Jacques Burger†

*Institut National de la Santé et de la Recherche Médicale U. 483, Université Pierre et Marie Curie, 75252 Paris Cedex 05, France; and †Laboratoire d'Ingéniérie des Systèmes Automatisés, Université d'Angers, 49000 Angers Cedex, France

ABSTRACT An electro-osmotic model is developed to examine the influence of plasma membrane superficial charges on the regulation of cell ionic composition. Assuming membrane osmotic equilibrium, the ion distribution predicted by Gouy-Chapman-Grahame (GCG) theory is introduced into ion transport equations, which include a kinetic model of the Na/K-ATPase based on the stimulation of this ion pump by internal Na^+ ions. The algebro-differential equation system describing dynamics of the cell model has a unique resting state, stable with respect to finite-sized perturbations of various types. Negative charges on the membrane are found to greatly enhance relaxation toward steady state following these perturbations. We show that this heightened stability stems from electrostatic interactions at the inner membrane side that shift resting state coordinates along the sigmoidal activation curve of the sodium pump, thereby increasing the pump sensitivity to internal Na^+ fluctuations. The accuracy of electrostatic potential description with GCG theory is proved using an alternate formalism, based on irreversible thermodynamics, which shows that pressure contribution to ion potential energy is negligible in electrostatic double layers formed at the surfaces of biological membranes. We discuss implications of the results regarding a reliable operation of ionic process coupled to the transmembrane electrochemical gradient of Na^+ ions.

INTRODUCTION

To maintain their functional integrity, cells must face a number of constraints, including osmotic ones. In particular, animal cells avoid osmotic lysis only because they can equalize osmotic pressure between the two sides of their membrane by actively pumping out Na^+ ions with an ionmotive pump, the Na/K-ATPase (Hoffman and Simonsen, 1989). Because of this pump-leak mechanism, regulation of cell volume is tightly coupled with that of membrane polarization and of ion concentrations. A further complication in this coupling arises from the electric double layers that are formed at the plasma membrane surface. The surface potential was shown thus to control activity of the Na/K-ATPase by changing the local concentration of its cationic substrates sodium and potassium (Ahrens, 1981, 1983) and its anionic ligands ATP, ADP, and Pi (Nørby and Essmann, 1997). In addition to their effects on specific molecular targets, numerous compounds, which are either endogenous or exogenous, modify charge distribution on the cell membrane surface and should thus affect activity of enzymes like the Na/K-ATPase. It is therefore likely that the surface potential represents an important factor in the control of ion processes and cell metabolism (Wojtczak and Naleçz, 1985). In this context it might be wondered whether electrostatic control of the Na/K-ATPase could bring about a functional advantage to living cells. In other words, in view of the fact that the function of the Na/K-ATPase is to regulate ion concentrations, could electrostatic interactions enhance the stability of these concentrations faced with naturally occurring perturbations?

Most existing models of cell electro-osmotic regulation cannot be used for a general study of this question because they were designed to investigate the properties of specific cell types. However, models like the ones proposed by Kabakov (1994) and Jakobsson (1980) reduce description of electro-osmotic regulation to the basic mechanism of ion pump-leak quoted above, and therefore keep an essentially general character. In principle, the influence of electrostatic interactions on membrane transport can be introduced into these models by substituting superficial ion concentrations for bulk ones into ion transport equations. However, this requires having at one's disposal a model of the surface potential coherent with the full set of properties to be described. Thus, the most obvious approach would be to use the Gouy-Chapman equation or its generalized formulation for electrolytes with mixed valences, the Grahame equation (Hille, 1992; McLaughlin, 1989; Grahame, 1947). Indeed, this theory provides a quantitative description of unspecific (i.e., electrostatic) effects of ionic strength on the activation of numerous ion channels (Hille, 1992) and on activation of the Na/K-ATPase (Ahrens, 1981, 1983). However, this theory describes the solvent as a uniform dielectric continuum and consequently predicts the osmolarity at the charged surface of a membrane should be in excess of a quantity $1/2\kappa^2\epsilon\phi_S^2$ with respect to the bulk osmolarity, with κ^2 denoting the inverse of the Debye length, ϵ the dielectric constant of the solution, and ϕ_S the surface potential (Winterhalter and Helfrich, 1988). Mechanical equilibrium of the electric double layer actually implicates establishment of an excess pressure at the charged interface (Sanfeld, 1968). One must therefore carefully evaluate to what degree this

Received for publication 19 October 2000 and in final form 17 August 2001.

Address reprint requests to Dr. Stephane Genet, INSERM U483, U.P.M.C., Boite 23, 9, quai Saint-Bernard, 75005 Paris, France. Tel.: 33-1-44-27-34-37; Fax: 33-1-44-27-34-38; E-mail: stephane.genet@snv.jussieu.fr.

0006-3495/01/11/2442/16 $2.00

pressure is challenging theoretical results derived from the application of the Gouy-Chapman-Grahame theory to biological membranes.

The paper is organized as follows. First, we cast equations describing the time evolution of ion concentrations, membrane potential, and volume of a model cell endowed with a superficially charged plasma membrane; the model is derived from Kabakov's (1994) and Jakobsson's (1980) studies and equations make use of the ion distribution predicted by Gouy-Chapman-Grahame theory. Next, we use irreversible thermodynamics (see Durand-Vidal et al., 2000; Sanfeld, 1968) to give a more general description of electrostatic potentials at the cell membrane surface by including pressure in ion potential energy. This formalism is used in the first Results section to show that Gouy-Chapman-Grahame theory provides a very good approximation of the electrostatic potential in an electric double layer where osmotic equilibrium is achieved. The reader most interested in the biophysics of the cell model should turn immediately to subsequent sections, where it is shown that the model admits a unique resting state, the stability of which depends on the presence of charges at the membrane surface. We show that negative charge densities, with values comparable to those found on biological membranes, greatly accelerate recovery of resting concentrations after various perturbations. A local stability analysis, shown in the Appendix, is used to show that this heightened stability stems from an increase in the Na/K-ATPase flux sensitivity to internal Na^+ ions induced by electrostatic interactions.

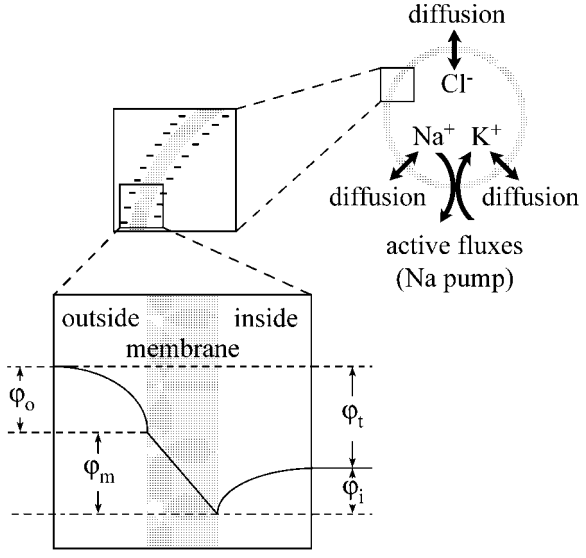

FIGURE 1 Structure of the model of electro-osmotic regulation within an animal cell. Regulations of cell volume and membrane polarization are coupled by the pump-leak mechanism, which renders the membrane functionally impermeable to Na^+ ions. Superficial charges of the membrane modify the ion distribution near the membrane sides. Concentrations appearing in ion transport equations are therefore superficial concentrations, as predicted by the Gouy-Chapman-Grahame theory of the electric double layer. Electrostatic potential φ_o at the membrane outer surface (minus the potential at infinite distance from the cell), the potential φ_i at the inner membrane side (minus the potential at the center of the cell), and the transmembrane potential (difference of potentials between the internal and external sides of the membrane) appear in equations as dimensionless potentials u, v, and w, respectively. It is assumed that the cell membrane remains in osmotic equilibrium and that both inner and outer compartments are electrically neutral at each moment.

MODEL CONSTRUCTION

Basic assumptions

Let us consider the cellular model schematized in Fig. 1 into which a cytoplasmic compartment is separated from the external milieu by a membrane charged on its two sides. The membrane is permeant to Na^+, K^+, and Cl^- ions, while the active fluxes of the Na/K-ATPase equilibrate the diffusional flux of each of the two cations. The cell also contains a fixed quantity, n_a, of impermeant monovalent anions and a fixed number, n_d, of divalent cations (we can readily identify the latter to Mg^{2+}, the major divalent cation type in animal cells). We first define the following dimensionless potentials:

$$u = \exp(-F\varphi_o/RT) \tag{1a}$$

$$v = \exp(-F\varphi_i/RT) \tag{1b}$$

$$w = \exp(-F\varphi_t/RT), \tag{1c}$$

where φ_o, φ_i, and φ_t denote electric potential differences depicted in Fig. 1. The macroscopic membrane potential difference φ_m, measurable with microelectrodes, is given by:

$$\varphi_m = \varphi_t + \varphi_o - \varphi_i. \tag{2}$$

We assume that membrane charges affect ion transport only through the following two processes:

1. Concentration of ion species j with valency z_j effectively "seen" by membrane structures of passive and active transport does not stand for the bulk concentration, but for concentration in the immediate vicinity of the membrane surface. If we put forward the hypothesis that quasi-equilibrium is achieved inside internal and external compartments at each point in time, these concentrations are related by the Maxwell-Boltzmann statistics:

$$[j]_{os} = [j]_o u^{z_j} \tag{3a}$$

$$[j]_{is} = [j]_i v^{z_j}, \tag{3b}$$

where $[j]_o$, $[j]_{os}$, $[j]_i$, and $[j]_{is}$, respectively, denote the concentration of species j in the bulk of external medium, at the external surface of the membrane, in the bulk of the cytoplasm, and at the internal side of the membrane.

2. Measured binding constants of the sodium pump with its ionized substrates are apparent constants (Nørby and Essmann, 1997; Ahrens, 1983). If we denote these by $K_j^{(a)}$ and thermodynamic constants by $K_j^{(T)}$, we have:

$$K_j^{(T)} = K_j^{(a)} u^{z_j} \tag{4a}$$

$$K_j^{(T)} = K_j^{(a)} v^{z_j}, \tag{4b}$$

if the binding site is either on the external side (Eq. 4a) or on the internal side of the membrane (Eq. 4b).

Constitutive equations of the model cell

If the small charge imbalance from which the membrane potential difference arises was omitted (see Roux, 1997), the principle of macroscopic electroneutrality would imply that the total charge in the cytoplasmic compartment was zero. Therefore, ions in the solution must equilibrate the intrinsic charges on the inner membrane side. Rapid estimate with typical cell radii, however, shows that this charge corresponds to a negligible number of ions compared to the total number of ions contained in cells. One can therefore approximate that the ion bulk concentration $[j]_i$ of an ion species j is related to the mole number n_j in the cell by:

$$[j]_i = n_j/V, \tag{5}$$

where V denotes the cell volume (m^3). Assuming that ion diffusion across the membrane obeys the constant field equation of Goldman (1943), the time evolution of the Na^+ and K^+ ion mole numbers in the cytoplasm follows the ordinary differential equations:

$$\frac{dn_{Na}}{dt} = \frac{P_{Na} \ln w}{1-w}\left(\frac{n_{Na}v}{V} - [Na]_o uw\right) - J^{(a)}_{Na} \tag{6}$$

$$\frac{dn_K}{dt} = \frac{P_K \ln w}{1-w}\left(\frac{n_K v}{V} - [K]_o uw\right) - J^{(a)}_{Na}/r_p \tag{7}$$

where $J^{(a)}_{Na}$ denotes the sodium pump active flux of Na^+ ions and r_p the coupling ratio of Na^+ on K^+ active fluxes, while P_{Na} and P_K denote the integrated permeability of the membrane ($m^3\ s^{-1}$) for Na^+ and K^+ ions, respectively. Flux $J^{(a)}_{Na}$ is given by:

$$J^{(a)}_{Na} = Q\alpha\beta, \tag{8}$$

where coefficient Q scales the maximum flux of the pump and where α and β are two functions with the range [0, 1], given by:

$$\alpha = \frac{[Na]_i^m v^m}{K_s^m + [Na]_i^m v^m} \tag{9a}$$

$$\beta = \frac{K_i^n}{K_i^n + [Na]_o^n u^n}\frac{[K]_o^q u^q}{K_c^q + [K]_o^q u^q} \tag{9b}$$

with:

$$K_i^n = U\left(1 + \frac{[K]_o^q u^q}{K_c^q}\right) w^{-\bar{z}_{Na}} \tag{9c}$$

where K_s, K_i, and K_c are ion binding constants (M), U a scaling factor, and $\bar{z}_{Na}$ the fraction of charge that raises the membrane electric field during deocclusion of Na^+ ions on the external side of the membrane; parameters m, n, and q are Hill coefficients. Equation 8 accounts for the independence of the effects of cationic substrates of the pump on the two sides of the membrane (Garay and Garrahan, 1973; Apell, 1989; Laüger, 1991). Equations 9, b and c are given by the model of Vasilets et al. (1993).

Jakobsson (1980) noticed that other processes involved in cell volume regulation are much faster than the time evolution of ionic concentrations. We can therefore assume that these processes remain in a pseudo-equilibrium state at each moment (see Appendix), and replace differential equations governing the evolution of fast variables with algebraic equations. Thus, we can assume macroscopic electroneutrality of the cytoplasm at each point in time which, from Eq. 5, gives:

$$n_{Na} + n_K + 2n_d = n_{Cl} + n_a, \tag{10}$$

from which we can deduce two more relations. First, we can write down a flux equation for Cl^- ions with the help of the Goldman equation. By introducing this equation in Eq. 10 and after differentiation with respect to time, we find that the w potential satisfies:

$$\frac{(1-w)(1+1/r_p)}{\ln w} + wu(P_{Na}[Na]_o + P_K[K]_o) - \frac{(P_{Na}n_{Na} + P_K n_K)v}{V} + P_{Cl}\left(\frac{wn_{Cl}}{Vv} - \frac{[Cl]_o}{u}\right) = 0. \tag{11}$$

Second, we assume that electrostatic potentials on the two membrane sides can be described with the Grahame (1947) equation. When considering a spherical cell, these equations write, with the help of Eq. 10:

$$\frac{Q_i^2 V^{-1/3}}{2\epsilon_0\epsilon_r RT(4\pi)^{2/3}3^{4/3}} - ((n_{Na} + n_K)(v + 1/v - 2) + n_d(v + 2/v - 3)) = 0, \tag{12}$$

for the internal compartment, and:

$$\frac{Q_0^2}{2\epsilon_0\epsilon_r RT(36\pi)^{2/3}V^{4/3}} - \sum_{\text{ions j}}[j]_o(u^{z_j} - 1) = 0, \tag{13}$$

for the outer solution; Q_i and Q_o denote the total charge on the internal and the external side of the membrane, respectively. Surface charges partly recombine with cations (McLaughlin et al., 1971), so that Q_o and Q_i are given by (Genet and Cohen, 1996):

$$Q_o = Q_{ot}\frac{1 + \sum_{\text{cations j}}(1 - z_j)[j]_o u^{z_j}K_j}{1 + \sum_{\text{cations j}}[j]_o u^{z_j}K_j} \tag{14a}$$

$$Q_i = Q_{it}\frac{1 - (v^2/V)K_d n_d}{1 + (v/V)(n_{Na} + n_K) + (v^2/V)K_d n_d}, \tag{14b}$$

where Q_{ot} and Q_{it} now denote the intrinsic amount of charges on the two sides of the membrane (i.e., without cations) and where the K_j values are thermodynamic binding constants (see Eq. 4).

As the Gouy-Chapman-Grahame theory neglects the excess mechanical pressure induced by ion accumulation at a charged interface, we can write that the osmolarity in the bulk of the cytoplasm remains identical to that in the bulk of the external medium in order for the membrane to be in osmotic equilibrium:

$$V[S]_o - (n_{Na} + n_K + n_d + n_{Cl} + n_a) = 0, \tag{15}$$

where $[S]_o = \Sigma_{\text{ionsj}}[j]_o$ is the bulk osmolarity in the external compartment.

Extension of the Gouy-Chapman-Grahame theory

The above equations make the basic assumption contained in the Gouy-Chapman-Grahame theory, which involves replacing the potential of mean force acting on ions with the mean electrostatic potential (see Durand-Vidal et al., 2000). To examine whether this assumption is physically consistent with the mechanical equilibrium of the membrane, we now give an alternate description of membrane electrostatic potentials, which introduces the mechanical excess pressure induced by electric fields at the charged membrane sides.

The Gibbs-Duhem equation for a polarized system (De Groot and Mazur, 1962, p. 397, Eq. 102) can be written with dimensions that allow one to have the chemical potentials, $\mu_i^{(m)}$, of the system components (i =

$1, \ldots, r$) expressed as molar quantities (J mol^{-1}):

$$\nabla p = S_v \nabla T + \sum_{i=1}^{r} C_i \nabla \mu_i^{(m)} + (\nabla \mathbf{E}) \cdot \mathbf{P}, \tag{16}$$

where T denotes the absolute temperature, p the pressure (N m^{-2}), S_v the entropy density (JK^{-1} m^{-3}), C_i the molar concentration of the component i (mol m^{-3}), $\mathbf{E}$ the electric field vector (V m^{-1}), and $\mathbf{P}$ the polarization density vector (C m^{-2}). $\mathbf{P}$ is related to the molar dipolar moment vector $\mathbf{P}_i^{(m)}$ (C m mol^{-1}) of the system components by:

$$\mathbf{P} = \sum_{i=1}^{r} C_i \mathbf{P}_i^{(m)}. \tag{17}$$

If we denote the vector sum of the external force density by $\mathbf{F}$(N m^{-3}), neglecting forces arising from the gravitational field, we have:

$$\mathbf{F} = \sum_{i=1}^{r} C_i (z_i F \mathbf{E} + (\nabla \mathbf{E}) \cdot \mathbf{P}_i^{(m)}). \tag{18}$$

By subtracting Eq. 18 from Eq. 16 we obtain:

$$\nabla p - \mathbf{F} = S_v \nabla T + \sum_{i=1}^{r} C_i (\nabla \mu_i^{(m)} - z_i F \mathbf{E}), \tag{19}$$

into which one recognizes the gradient of electrochemical potential $\tilde{\mu}_i^{(m)}$:

$$\nabla \tilde{\mu}_i^{(m)} = \nabla \mu_i^{(m)} - z_i F \mathbf{E}. \tag{20}$$

At thermal equilibrium ($\nabla T = 0$), the condition to have mechanical equilibrium of a volume element is that:

$$\nabla p - \mathbf{F} = 0, \tag{21}$$

and thereby, that electrochemical potential gradients simultaneously vanish for all species comprising the system:

$$\nabla \tilde{\mu}_i^{(m)} = 0, \quad i = 1, \ldots, r. \tag{22}$$

Given the hypothesis of local equilibrium, $\nabla \mu_i^{(m)}$ writes (De Groot and Mazur, 1962):

$$\nabla \mu_i^{(m)} = -\bar{s}_i \nabla T + \bar{v}_i \nabla p - (\nabla \mathbf{E}) \cdot \mathbf{P}_i^{(m)} + \sum_{i=1}^{r} \frac{\partial \mu_i^{(m)}}{\partial N_j} \nabla N_j, \tag{23}$$

where N_i, $\bar{v}_i$, and $\bar{s}_i$ respectively denote the mole fraction, the partial molar volume (m^3 mol^{-1}), and the partial molar entropy (JK^{-1} mol^{-1}) of component i, which are defined with the usual thermodynamic relations:

$$\left(\frac{\partial \mu_i^{(m)}}{\partial p} \right)_{T,N_i} = \bar{v}_i \tag{24a}$$

$$\sum_{i=1}^{r} C_i \bar{v}_i = 1 \tag{24b}$$

$$\left(\frac{\partial \mu_i^{(m)}}{\partial T} \right)_{p,N_i} = -\bar{s}_i \tag{24c}$$

$$\sum_{i=1}^{r} C_i \bar{s}_i = S_v \tag{24d}$$

The sum in Eq. 23 represents the contribution to $\nabla \mu_i^{(m)}$ of the ith component and of its interactions with the other components. From statistical mechanics, the former can be shown to obey:

$$\frac{\partial \mu_i^{(m)}}{\partial N_i} = RT/N_i. \tag{25}$$

Finally, the electric field $\mathbf{E}$ must satisfy the Poisson equation from electrostatics:

$$\epsilon_o \nabla \cdot (\epsilon_r \mathbf{E}) = F \sum_{i=1}^{r} z_i C_i, \tag{26}$$

where ϵ_o (F m^{-1}) is the permittivity of vacuum, and ϵ_r the dielectric constant. Recall that:

$$C_i = N_i \Big/ \sum_{i=1}^{r} N_i \bar{v}_i. \tag{27}$$

Following the Gouy-Chapman theory assumptions, we neglect intermolecular interactions in Eq. 23, so that, at thermal equilibrium, Eq. 22 becomes:

$$\bar{v}_i \nabla p - (\nabla \mathbf{E}) \cdot \mathbf{P}_i^{(m)} + \frac{RT}{N_i} \nabla N_i - z_i F \mathbf{E} = 0, \quad i = 1, \ldots, r. \tag{28}$$

We also assume 1) that ϵ_r has a uniform value, so that Eq. 26 now reads:

$$\nabla \cdot \mathbf{E} = \frac{F \sum_{i=1}^{r} z_i N_i}{\epsilon_o \epsilon_r \sum_{j=1}^{r} N_j \bar{v}_j}, \tag{29}$$

and 2) that the solvent (referred to by subscript 1) is the only component having a dipolar moment given by:

$$\mathbf{P}_1^{(m)} = \mathbf{P}/C_1 = (\epsilon_0 \chi \mathbf{E})/C_1 \tag{30}$$

if one neglects dielectric saturation (Eyges, 1980); $\chi = \epsilon_r - 1$ denotes the electric susceptibility. Given that the electric double-layer thickness is negligible compared to the curvature radius of any cell, we apply these equations to a plane surface of infinite lateral extension normally oriented to the x-axis and in contact with a solution of a 1:1 electrolyte. Subscript 2 refers to the cation and subscript 3 to the anion, and the origin of the x-axis is put on the surface; the surface bears uniformly smeared charges with density σ (C m^{-2}). By noting that the sum of mole fractions is 1, that $\mathbf{E}$ is related to the electric potential φ by $\mathbf{E} = -\nabla \varphi$, and that the problem is monodimensional, we can write Eq. 28 explicitly for the three species composing the solution and Eq. 29 in terms of φ to obtain the following system of equations:

$$\bar{v}_1 \frac{dp}{dX} = \frac{\chi RT}{\epsilon_r} \frac{N_3 - N_2}{1 - (N_2 + N_3)} \frac{dY}{dX} + \frac{RT}{1 - (N_2 + N_3)} \frac{d}{dX} (N_2 + N_3) \tag{31a}$$

$$\frac{RT}{N_2} \frac{dN_2}{dX} = -\bar{v}_2 \frac{dp}{dX} - RT \frac{dY}{dX} \tag{31b}$$

$$\frac{RT}{N_3} \frac{dN_3}{dX} = -\bar{v}_3 \frac{dp}{dX} + RT \frac{dY}{dX} \tag{31c}$$

$$\frac{d^2 Y}{dX^2} = \frac{N_3 - N_2}{1 + N_2(\bar{v}_2/\bar{v}_1 - 1) + N_3(\bar{v}_3/\bar{v}_1 - 1)} \tag{31d}$$

which was recast into nondimensional form by introducing the reduced variables:

$$Y = \frac{F\varphi}{RT} \tag{32a}$$

and

$$X = \lambda x \tag{32b}$$

with

$$\lambda^2 = \frac{F^2}{\epsilon_0\epsilon_r RT\bar{v}_1}. \tag{32c}$$

In addition to equation system 31, we have the following boundary conditions:

$$\lim_{X\to\infty} N_2(X) = \lim_{X\to\infty} N_3(X) = N_0 \tag{33a}$$

$$\lim_{X\to\infty} Y(X) = 0 \tag{33b}$$

$$\lim_{X\to\infty} \frac{dY}{dX}(X) = 0 \tag{33c}$$

$$\lim_{X\to\infty} p(X) = 0, \tag{33d}$$

whereas Gauss theorem together with the condition of electroneutrality of the charged plan-solution set allows us to establish that:

$$\frac{dY}{dX}(X=0) = \frac{\sigma F}{\lambda\epsilon_0\epsilon_r RT}. \tag{33e}$$

We recall finally that the Gouy-Chapman equation writes:

$$\frac{d^2Y}{dX'^2}(X') = \sinh Y(X'), \tag{34}$$

where $X' = \kappa x$ with

$$\kappa^2 = \frac{2F^2C_0}{\epsilon_0\epsilon_r RT}, \tag{35}$$

with boundary conditions:

$$\lim_{X'\to\infty} Y(X') = \lim_{X'\to\infty} \frac{dY}{dX'}(X') = 0 \tag{36a}$$

$$\frac{dY}{dX'}(X'=0) = \frac{\sigma F}{\kappa\epsilon_0\epsilon_r RT} \tag{36b}$$

Parameters

Equations 12 and 13 are written in terms of Q_{ot} and Q_{it} rather than charge densities, because the latter change with cell volume. However, physiological perturbations of cell ionic composition occur on much shorter time scales than the turnover of membrane components. The intrinsic charge of the membrane can therefore be considered constant for the study of such perturbations. It was expressed as a multiple of a reference value $Q_{ref} = 1.0 \times 10^9$ e by defining the ratio $\theta = Q_{ot}/Q_{ref}$. Similarly, we introduce the ratio $\gamma = Q_{it}/Q_{ot}$ to study the effects of the relative proportion of charges between the two membrane sides. This model describes transport of Na^+, K^+, and Cl^- ions only. Thus, any discrimination between other ion species excepted on the basis of their electric valency or binding constant with surface charges is irrelevant. Nevertheless, we will refer to divalent cations as to calcium ions, which are the major divalent species in the extracellular space. The reference composition for the external solution was (in mM): $[Na]_o = 120$, $[K]_o = 5$, $[Ca]_o = 2.5$ with osmolarity adjusted to 310 mM with the chloride salt of a monovalent cation inert with respect to membrane ion transport. Other parameters are listed in Table 1.

TABLE 1 Parameters for the simulation of the reference model

$1/(2\epsilon_0\epsilon_r RT)$	265 e^{-2} $MÅ^{-4}$ at $T = 310.15$ K
P_{Na}	4×10^{-14} cm^3 s^{-1}*
P_K	4×10^{-13} cm^3 s^{-1}*
P_{Cl}	4×10^{-13} cm^3 s^{-1}*
Q	2×10^{-13} M s^{-1}*
K_s	22.49 mM†
K_c	1.58 mM†
K_i	1440 mM at $\varphi_t = 0$ mV‡
$\bar{z}_{Na}$	0.5‡
m	3.0†§
n	1.6‡
q	1.3¶
U	25990 M^{-n} deduced from other parameters using Eq. 9c
$K_K = K_{Na}$	$0.15M^{-1}$‖
K_d	$2.25M^{-1}$‖
r_p	−3/2

*From Jakobsson (1980).
†From Jewell and Lingrel (1991).
‡From Vasilets et al. (1993).
§From Garay and Garrahan (1973).
¶From Rakowski et al. (1991).
‖From Cevc (1990).

Numerical methods

Most computations with the algebro-differential system 6, 7, 10, 11, 12, 13, 15 were performed with MAPLEV, using the ODE/DAE solver BESIRK for its integration.

Integration of equation system 31 presented a basic difficulty, as the system is associated to boundary conditions on the charged plane and at infinite distance (Eqs. 33, a–e), whereas numerical procedures require a finite interval. Several strategies allow bypassing this problem but they present difficulties (see Stafiej et al., 1996). We therefore followed the approach of Forsten et al., (1994) by simply truncating the infinite interval at length L to rewrite condition 33b on Y at $X = L$; equations were integrated either with the shooting method capability of the XPP software or a P1 finite element method, the two methods giving closely matching results. Truncating the integration interval prevented the condition of zero electric field to be strictly satisfied at $X = L$ and, due to this approximation, the solution proved highly sensitive to the interval length for small L values. But above $L = 30$, the surface potential $Y(X = 0)$ adopted an asymptotic behavior, its value changing only on the fourth decimal for small increments in the interval length above $L = 50$. The following partial volumes of monovalent cations were used for computations: $\bar{v}_1 = 18 \times 10^{-6}$ m^3 mol^{-1}; $\bar{v}_2 = \bar{v}_3 = 25 \times 10^{-6}$ m^3 mol^{-1}. For comparison with the Grahame equation, the partial volume of divalent cations was given values, ranging from one to three times that given to monovalent ions, that induce negligible incidence on the difference between the solution of Eqs. 31 and that of Eq. 34.

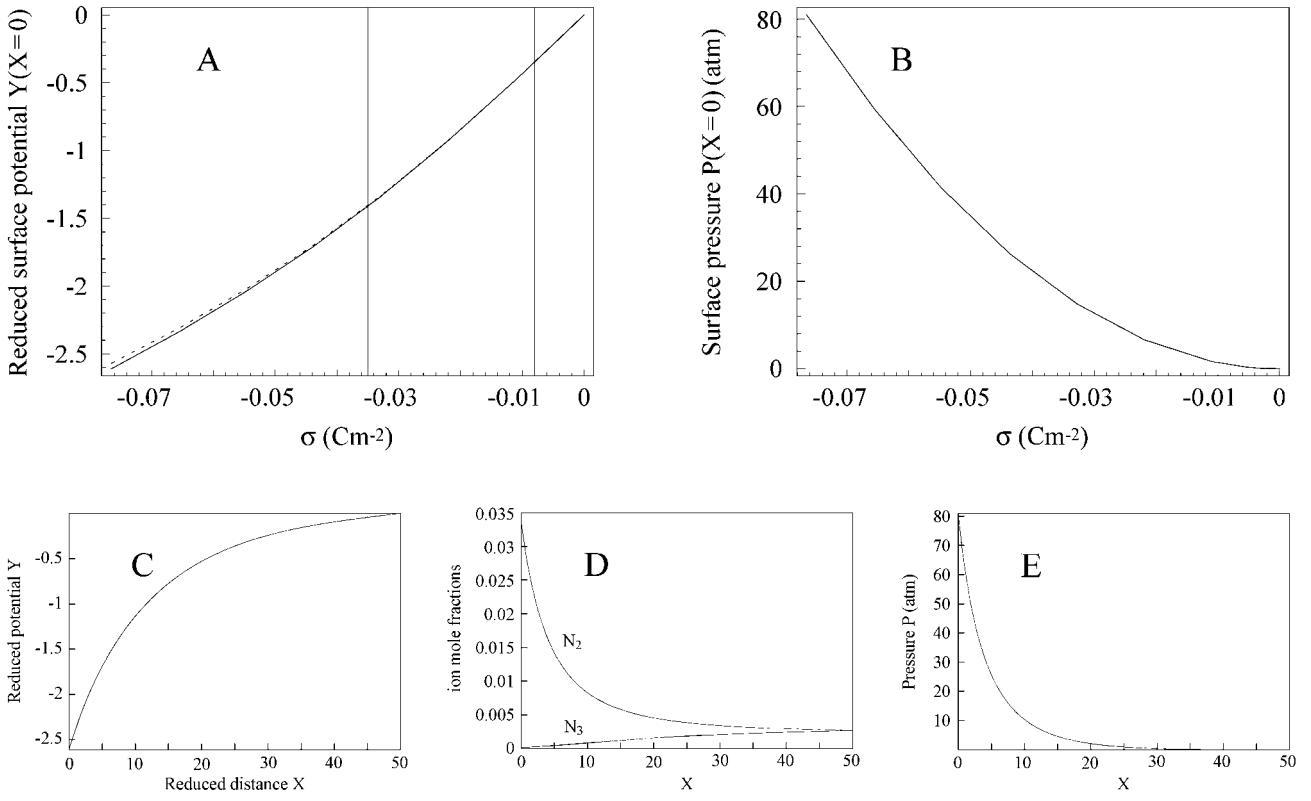

FIGURE 2 Comparison between TIP equations (Eq. 31) and the Gouy-Chapman theory (Eq. 34) for description of electrostatic potential in the electric double layer. (*A*) Reduced surface potential $Y(X = 0)$ versus surface charge density σ according to Eq. 31 (*solid line*) and Eq. 34 (*dotted line*); (*B*) pressure on the charged plane predicted by TIP equations. Lower graphs illustrate profiles of reduced potential (*C*), ion mole fractions (*D*), and pressure (*E*) versus reduced distance from the charged plane, as given by TIP equations for $\sigma = -0.0765$ Cm^{-2}. All data were computed for a 150 mM solution of a 1-1 electrolyte (N_2 and N_3 denote mole fractions of the anion and the cation, respectively). The two vertical lines in graph (*A*) delimit the interval of mean charge densities measured at the surface of biomembranes (-0.035, -0.008 Cm^{-2}; Wojtczak and Naleçz, 1985).

RESULTS

Adequacy of the Gouy-Chapman-Grahame theory to describe membrane electrostatic potentials

Fig. 2 compares the numerical solution of the TIP equations (Eq. 31) to the analytical solution of the Gouy-Chapman equation (Eq. 34) as functions of σ for $N_0 = 0.0027$ (giving a concentration $C_0 \simeq 150$ mM, which corresponds well to that of the intracellular milieu). Graph *A* compares values of the reduced surface potential given by the two equations, while graph *B* gives pressure values at the charged plane as predicted by system 31. In the interval of compiled estimations for mean charge density on biological membranes (delineated by the two vertical bars on graph *A*), the two equations give the same surface potential within 0.1%. The region of larger charge densities in graph *A* reveals that the surface potential predicted by system 31 is, in fact, slightly more negative than the one given by the Gouy-Chapman equation, the difference increasing with charge density. This difference is due to the excess pressure, which ensures the mechanical equilibrium of the electric double layer (graph *B*); this pressure limits accumulation of cations at the charged wall, thereby reducing the screening of surface charges. However, the difference only amounts to 2% with the highest charge density used, $\sigma = -0.0765$ C m^{-2}, for which the profiles of the variables of system 31 are illustrated on graphs *C*, *D*, and *E* of Fig. 2. Because biological solutions comprise divalent cations, we also applied the TIP equations to a solution of electrolytes with mixed valences to compare it with the Grahame equation (Grahame, 1947), which relies on the same basic assumptions as the Gouy-Chapman theory. Again, results did not differ by $>2\%$ within the millimolar range of divalent cation concentrations encountered in biological media (not illustrated).

These results confirm Laüger et al.'s (1967) insight that the influence of pressure on ion potential energy in the double layer is negligible in the range of parameter values corresponding to biological membranes. Within this range, the Gouy-Chapman-Grahame theory therefore provides a reliable approximation of the electric potential profile at a single charged interface, where all components in the solution, including the solvent, are in thermodynamic equilibrium. However, biomembranes achieve two such interfaces. Thus, it follows that, in addition to conditions of the type

33e on the electric field, continuity conditions on the electric displacement also hold at the membrane boundaries. These conditions entail an electrostatic coupling across the membrane, the intensity of which depends both on the membrane specific capacitance and magnitude of the transmembrane electric potential difference (Genet et al., 2000). Here, we suppose that this difference is not too large (absolute value <100 mV). Thus, and given that the capacitance of the double layers is larger than that of the membrane, the electrostatic coupling can be neglected (see Peitzsch et al., 1995). In contrast, a pressure discontinuity will occur across the membrane in the case of unequal charge densities on the two membrane sides. However, because solute activity coefficients are ignored in the Gouy-Chapman-Grahame theory, the solvent chemical potential profile will be uniform across the membrane, thereby guaranteeing membrane osmotic equilibrium, providing the bulk osmolarity is the same in the two solutions that are in contact with the membrane boundaries.

Resting point of the model

Three distinct stationary points were found for $-5 < \theta < 1$ and $0.1 < \gamma < 1.3$ with the reference value of other parameters. Existence of multiple stationary points is due to Eqs. 12 and 13, which involve the square of Q_{ot} and of Q_{it}. One therefore finds solutions corresponding to the sign given to these parameters and nonphysical solutions corresponding to the opposite sign. Two of the points found correspond to such nonphysical states, whereas the third one appears consistent with the sign chosen for Q_{ot} and Q_{it}. Fig. 3 illustrates dynamics of the model following three distinct perturbations of its stationary state in the case where $\theta = -1.5$ and $\gamma = 1$; that is, for a symmetrical distribution of negative charges on the two membrane sides. These perturbations consisted of changing the value of a single parameter and then finding coordinates of the corresponding resting state. These were used as initial conditions for the integration of equations with the reference value of the parameters. Illustrated perturbations are a partial neutralization of charges on the inner side of the membrane, an increased P_{Na} and an increased $[K]_o$. In all cases, the model consistently relaxed toward the same resting point.

Furthermore, we found the model to admit a resting state with physical significance in an extended range of ionic compositions of the external medium (hypo/hyperkalemia ($2 < [K]_o < 8$ mM), hypo/hypernatremia ($100 < [Na]_o < 150$ mM), and hypo/hypercalcemia ($2 < [Ca]_o < 20$ mM), as well as for significant departures from the reference value of all other parameters. In every case, the model converged to the resting point following finite perturbations of the kind illustrated in Fig. 3.

As there was no sign suggesting existence of a limit cycle, we can assume that the model has a unique resting point because nonphysical points were never reached as long as consistent initial conditions were chosen for integrating equations. Moreover, the above results cover a priori the range of parameter values corresponding to pathophysiological situations. This suggests strongly that the stationary state is globally stable even if formal demonstration of this property would require finding a Lyapunov function for the model under investigation.

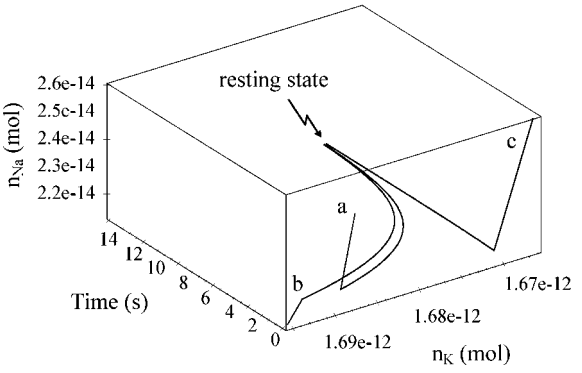

FIGURE 3 Trajectories of the model following three different perturbations of its resting state. Curves show the time evolution of Na^+ and K^+ ions' mole numbers in the cell with parameters set at their reference value (Table 1), and membrane charge distribution set by $\theta = -1.5$ and $\gamma = 1$ (i.e., with negative charges symmetrically distributed between the two membrane sides). Initial conditions for each curve corresponded to the resting state coordinates of the model with one of its parameters changed from its reference value: (*a*) $P_{Na} \times 1.2$ (increased sodium permeability); (*b*) $[K]_o = 7$ mM (hyperkalemia); (*c*) $Q_{it} \times 0.8$ (partial neutralization of charges on the inner membrane side). The system also converged toward the same steady state with all types of perturbations tested, and qualitatively identical results were obtained with different charge distributions on the membrane.

Negative charges on the membrane increase the resting state stability

We examined the influence of membrane charges on the model dynamics by integrating the equation system with various assumptions on charge distribution for several sets of initial conditions departing from the resting state. Fig. 4 displays an example where the initial state presented an increased n_{Na} and a decreased n_K by 5×10^{-15} mol, corresponding to a 0.4 mM deviation from resting value in each of the two cation concentrations. This perturbation simulates ion composition changes that neurons withstand following a brief, sustained discharge of action potentials. Rather than plotting absolute values of state variables, we have represented their deviations from resting value to highlight the influence of membrane charges on the rate of relaxation.

The top half of Fig. 4 displays relaxation curves of sodium (*A*) and potassium (*B*) concentration deviations for various amounts of charges distributed symmetrically on the two membrane sides (i.e., $\gamma = 1$). With an uncharged membrane ($\theta = 0$, *thick curves*), cation concentrations have only slightly changed at the end of the illustrated time

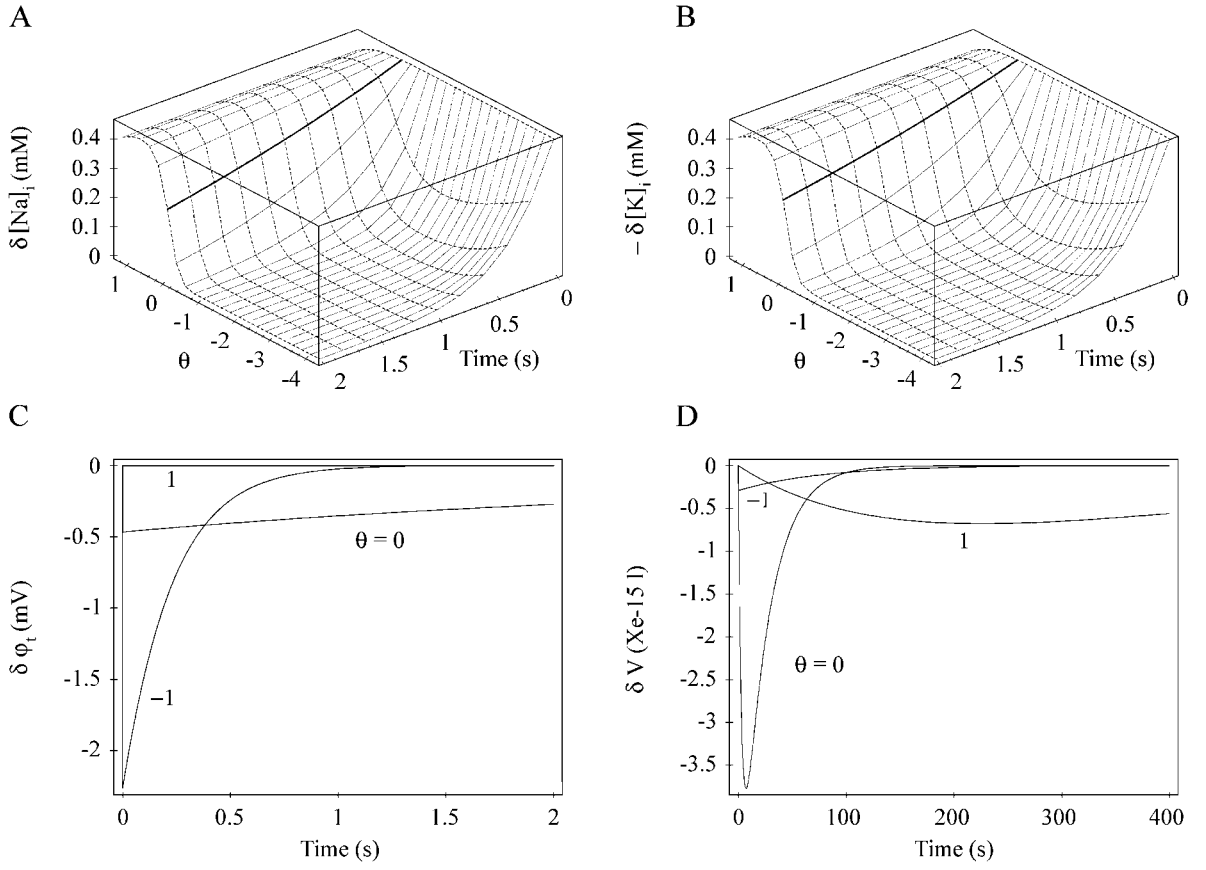

FIGURE 4 Influence of membrane charges on the rate of relaxation of the model following a perturbation of its internal ionic composition. Perturbation consisted in increasing n_{Na} by 5×10^{-15} mol and decreasing n_K by the same amount from resting values. To highlight membrane charge effects, graphs display the time evolution of deviations of the model variables with respect to their resting values. (*A*) internal sodium concentration $[Na]_i$. (*B*) Internal potassium concentration $[K]_i$; the negative of the cation concentration deviation is plotted for comparison with (*A*). (*C*) Transmembrane potential φ_t. (*D*) Cell volume *V*. For these simulations, membrane charges were equally distributed between the two membrane sides, by setting $\gamma = Q_{it}/Q_{ot}$ to 1, while their density was varied by changing $\theta = Q_{ot}/Q_{ref}$ ($Q_{ref} = 1.0 \times 10^9$ e); thick curves correspond to the neutral membrane case. Note the prominent increase in the rate of relaxation of Na^+ and K^+ induced by negative membrane charges.

interval of 2 s (full recovery took ~30 s); but negative charges on the membrane speed up relaxation at such a point that both concentrations have fully resumed their resting value after the same time span for $-4 < \theta < -1$. Dashed curves that connect relaxation curves at several discrete times give clear evidence that a maximum rate of relaxation occurs around $\theta = -2$. Positive charges exert an opposite influence, but it is barely perceptible on the graphs (a shorter interval of integration would have highlighted this effect, but it would have prevented a better resolution of the curve for $\theta < 0$). It is interesting that even though P_{Na} is 10 times smaller than P_K, membrane charges about equally change the relaxation rate of the two cation concentrations. This evidently points the origin of membrane charge effects on the rate of relaxation to the process of ion active transport by the sodium pump, rather than to passive ion fluxes.

The bottom half of Fig. 4 plots three significant samples of the transmembrane potential (*C*) and cell volume (*D*) relaxation curves corresponding to upper ion concentration curves. The membrane potential curve for a neutral membrane ($\theta = 0$) exhibits a transient 0.5 mV hyperpolarization, whose rate of decay matches that of cation concentration deviations on graphs *A* and *B* (*thick curves*). Membrane charges profoundly changed the magnitude and temporal pattern of this transient hyperpolarization. Its amplitude was larger (>2 mV) with negative charges ($\theta = -1$) on the membrane while it decayed much faster, with about the same kinetics than cation concentrations on top of the figure. With positive charges ($\theta = 1$), the hyperpolarization became so small (<0.01 mV) that the curve confounds with baseline potential, but its decay was very much prolonged with respect to the neutral membrane case, like that of cation concentrations on graphs *A* and *B*. This transient hyperpolarization unambiguously arose from a stimulation of the electrogenic sodium pump by the perturbation that had increased $[Na]_i$. Graph *C* therefore shows that this stimulation was larger with negative charges on the membrane than without, the pump stimulation becoming extremely

weak with positive charges. This again suggested that the origin of increased rate of recovery of cation concentrations induced by negative charges should reside in a modulation of the sodium pump activity by electrostatic interactions.

The cell model also underwent a transient shrinkage during relaxation toward steady state (Fig. 4 *D*). This shrinkage represents no more than a fraction of a percent change in resting volume ($V \simeq 0.108 \times 10^{-4}$ μl), owing to the initial internal osmolarity having the same 310 mM value than in the steady state. This transient shrinkage can be related to the sodium pump activation identified above, as this pump moves three Na^+ ions from the inside of the cell to the outside for two K^+ ions in the opposite direction; its sudden activation must therefore result in a small ion flux imbalance that transiently lower internal osmolarity. Consistent with this interpretation, the lower activation of the sodium pump found with positive charges on the membrane resulted in slower rise and decay of the transient shrinkage (curve labeled $\theta = 1$ on graph *D*). However, negative charges would have been expected to increase both amplitude and rate of decay of the cell shrinkage, whereas the curve labeled $\theta = -1$ on graph *D* exhibits just the opposite. This suggested that some factor may have prevented negative charges to accelerate relaxation of the cell volume like that of cation concentrations and membrane potential. The most likely candidate for such a factor was the chloride permeability P_{Cl}, as temporal changes of $[Cl]_i$ mirrored that of cell volume in all simulations (not illustrated). Thus, negative charges on the membrane resulted in faster cell volume transients changes than without charges when P_{Cl} was raised to 100 times its reference value (not illustrated). Most interestingly, curves of cation concentration relaxation remained almost identical to those illustrated in Fig. 4, whether P_{Cl} was given 10 or 100 times its reference value. This result agrees well with Jakobsson's (1980) simulations, which show that the magnitude of P_{Cl} weakly affects temporal changes in Na^+ and K^+ concentrations. Moreover, qualitatively similar data were obtained with much larger (up to several mM) deviations in cation concentrations for the specific perturbation illustrated in Fig. 4, as well as with other kinds of perturbations, such as those illustrated in Fig. 3. Overall, negative charges on the membrane consistently heightened the stability of resting cation concentrations, despite the fact that they had adverse effects on cell volume, depending on the magnitude of P_{Cl}.

Mechanism of heightened stability induced by negative membrane charges

To understand the origin of membrane charge effects on the cell model dynamics, we examined the local stability of the model in a neighborhood of its resting state. The Appendix shows that stability analysis can be reduced to that of a two-dimensional model with mole numbers n_{Na} and n_K as variables. Absolute value of the eigenvalues of the Jacobian matrix **J** of this system, evaluated at the resting state coordinates, are the reciprocal of the two characteristic times of relaxation of the model. The three-dimensional plots in Fig. 5 illustrate how these eigenvalues depended on the density of charges on the membrane (set by θ) and on their partition between the two membrane sides (set by γ). First, one sees that both eigenvalues were real and negative-valued across the entire domain of the (θ, γ) plane considered; this proves that the resting point is asymptotically stable over a broad range of the parameter values that set membrane charge distribution. Second, one can see from the different vertical scales on the two graphs of Fig. 5 that the model has two broadly different relaxation times. The λ_1 eigenvalue corresponds to short times ranging from tenths of seconds to seconds, while λ_2 corresponds to time scales ~100 times larger.

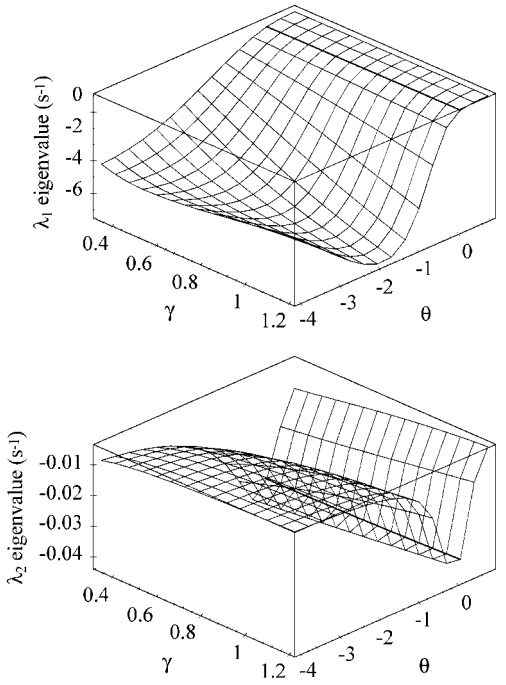

FIGURE 5 Membrane charge effects on the eigenvalues of the Jacobian matrix of equation system 6, 7 evaluated at the resting state. The absolute values of these eigenvalues are the reciprocal of the two characteristic times governing the rate of relaxation of the model following perturbations of its resting state (see Appendix). Parameter $\theta = Q_{ot}/Q_{ref}$ ($Q_{ref} = 1.0 \times 10^9$ e) sets the algebraic value of membrane charges, while parameter $\gamma = Q_{it}/Q_{ot}$ sets their distribution between the two membrane sides. The resting state is always stable with all charge distributions (both eigenvalues are strictly negative).

It is clear from Fig. 5 that membrane charges exert adverse influences on the two eigenvalues, and hence on the two relaxation times of the model. On the one hand, positive charges ($\theta > 0$) render λ_1 less negative than when the membrane bears no charge, thereby lengthening the short relaxation time. Negative charges ($\theta < 0$) have opposite and much more marked effects on this relaxation time, which can be reduced from ~3 s, with no membrane charges, down to 150 ms with $\theta = 2$ and $\gamma = 1.2$ (Fig. 5, *upper graph*).

On the other hand, both negative and positive charges render λ_2 less negative and therefore lengthen the long relaxation time of the model. For example, this relaxation time, which is ~25 s with no charge on the membrane, is increased to >100 s by the large density of negative charges ($-4 < \theta < -2$), whatever their distribution between the two membrane sides.

In principle, the overall degree of stability of the model is determined by the eigenvalue with the largest algebraic value, that is, λ_2 (see Bourlès, 1986). The λ_2 plot in Fig. 5 would therefore suggest that membrane charges, whatever their sign, should destabilize the resting point, but the above simulations have highlighted an increase in stability induced by negative charges, which is in better agreement with charge effects on λ_1. This suggested that relaxation velocity of the model depends mostly on λ_1. This was confirmed by further calculations showing that λ_2 contributes 100 times less than λ_1 to the rate of relaxation of the Na^+ and K^+ concentrations. Moreover, this conclusion agrees with the minimum in λ_1 for $\gamma = 1$, which occurs precisely for $\theta = -2$ (Fig. 5), like the maximum rate of recovery of ion concentrations found in Fig. 4. This feature of the model stems from the fact that negative charges shorten the relaxation time corresponding to λ_1 so much that the model has already almost fully recovered its resting state when its dynamics becomes dominated by λ_2.

Nevertheless, Fig. 5 also evidences that the way negative charges are distributed between the two membrane sides strongly influences their effect on the model stability. Thus, for $\theta < 0$ down to -2, λ_1 is more negative when charges concentrate on the inner side of the membrane ($\gamma = 1.2$). This tendency is inverted below $\theta = -2$ approximately, due to the existence of a minimum in the λ_1 curves as functions of θ with γ constant. This minimum, which is very pronounced for large γ values, is progressively shifted toward more negative θ values when γ is diminished, and thus that charges are less concentrated on the inner membrane side. This suggested that negative charges increased the model stability by a mechanism that principally involves electrostatic interactions at the inner membrane side.

Fig. 6 *A* shows, with the example of $\gamma = 1$, that the resting cell volume is largely insensitive to the membrane charge density, but membrane charges have profound effects on the bulk value of sodium concentration $[Na]_i$ and its local value $[Na]_{is}$ at the inner membrane surface. Thus, $[Na]_i$ tends to explode with growing density of positive charges, while growing density of negative charges consistently lowers the cation concentration. It is interesting that membrane charges have strictly opposed effects on $[Na]_{is}$ because these strictly follow changes on the sodium pump rate on graph *A*. Thus, the pump turns only at 6% of its maximum activity with no charges on the membrane, whereas it is activated at 60% for $\theta = -2$, the rate becoming extremely low with positive charges (graph *A*). The explanation for these rate changes lay in electrostatic interactions at the inner membrane side. By attracting cations, negative charges increase $[Na]_{is}$ and thereby stimulate the sodium pump (cf. Eq. 9a), which can achieve lower bulk Na^+ concentrations in the resting state than without charges on the membrane. This higher rate of active ion pumping explains the increased rate of relaxation induced by negative charges on the membrane. It equally explains the preponderant influence of inner membrane charges because internal sodium is the major regulation factor of the sodium pump. However, this mechanism does not explain why a maximal stability occurs at a precise density of negative charges (see Fig. 4), because the flux of the sodium pump, $J^{(a)}_{Na}$, on graph *A* increases monotonically with this density.

We could obtain a deeper understanding of this effect by analyzing the properties of the λ_1 eigenvalue. The characteristic equation for **J** writes:

$$\lambda^2 - \mathrm{tr} \cdot \lambda + \Delta = 0, \tag{37}$$

where

$$\mathrm{tr} = \frac{\partial \bar{F}_1}{\partial n_{Na}} + \frac{\partial \bar{F}_2}{\partial n_K} \quad \text{and} \quad \Delta = \frac{\partial \bar{F}_1}{\partial n_{Na}} \frac{\partial \bar{F}_2}{\partial n_K} - \frac{\partial \bar{F}_1}{\partial n_K} \frac{\partial \bar{F}_2}{\partial n_{Na}},$$

respectively, denote the trace and the determinant of **J** (see Appendix). For all charge distributions considered in this study, simulations showed that the second term of the right-hand side of Δ is at least two orders of magnitude smaller than the first term. We can therefore approximate λ_1 by:

$$\lambda_1 = \frac{\partial \bar{F}_1}{\partial n_{Na}}. \tag{38}$$

The $\partial f_1/\partial n_{Na}$ derivative accounts for 99% of the sum of terms that compose $\partial \bar{F}_1/\partial n_{Na}$, and the $\partial J^{(a)}_{Na}/\partial n_{Na}$ term dominates the sum of terms that compose $\partial f_1/\partial n_{Na}$ itself. According to Eq. 38 we may therefore write:

$$\lambda_1 \simeq -\frac{\partial J^{(a)}_{Na}}{\partial n_{Na}} = -\underbrace{\frac{QmK^m_s n^m_{Na} v^m/V^m}{n_{Na}(K^m_s + (n_{Na}v/V)^m)^2}}_{a_1(v)} \cdot \underbrace{\frac{K^n_i [K]^q_o u^q}{(K^n_i + [Na]^n_o u^n)(K^q_c + [K]^q_o u^q)}}_{a_2(u)}. \tag{39}$$

Graph *C* in Fig. 6 shows that λ_1 is well approximated by $-\partial J^{(a)}_{Na}/\partial n_{Na}$. This shows that negative charges increase the stability degree of the resting state by enhancing the sodium pump sensitivity to n_{Na} or, more generally, to $[Na]_i$, because cell volume was not significantly affected. Equation 39 exemplifies that charge effects on the sodium pump sensitivity to $[Na]_i$ can be split into an inner charge contribution (a_1) and an outer charge contribution (a_2). As seen from graph *D*, outer charges have almost no effect on the changes of sensitivity of the pump, as a_2 undergoes only a very slight and monotonic decrease when the density of negative charges is increased. How-

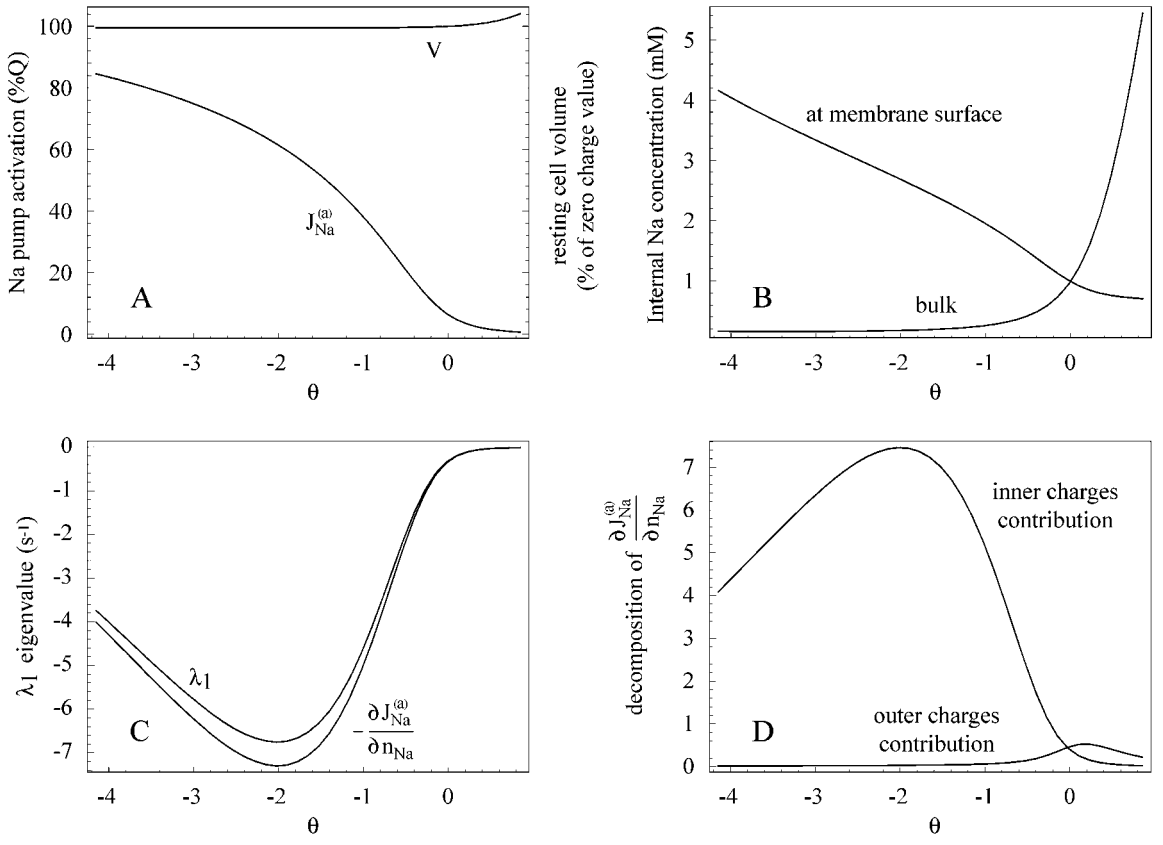

FIGURE 6 Mechanism of the heightened stability induced by negative membrane charges. Graphs display the influence of membrane charges on the activation of the sodium pump and related variables. (*A*) Sodium pump flux $J_{Na}^{(a)}$ (expressed as percent of maximum flux Q) and cell volume V. (*B*) Internal sodium concentration in the core of the cytoplasm, $[Na]_i$, and at the inner membrane side, $[Na]_{is}$. (*C*) λ_1 eigenvalue of equation system 6, 7 and negative of the sodium pump flux sensitivity to internal Na^+ ions, $-\partial J_{Na}^{(a)}/\partial n_{Na}$. (*D*) Splitting of inner and outer charge effects on $\partial J_{Na}^{(a)}/\partial n_{Na}$, according to Eq. 39. Negative charges increase $[Na]_{is}$, thereby stimulating the sodium pump, which can in turn achieve lower $[Na]_i$ levels in the resting state (*A*). The resulting changes in $\partial J_{Na}^{(a)}/\partial n_{Na}$ explain most of the influence of membrane charges on the λ_1 eigenvalue and hence on the stability of the resting state (*C*). Graph (*D*) shows that the overall effect primarily arise from electrostatic interactions at the inner membrane side. Parameter γ was set to 1 in this simulation.

ever, the inner charge depending factor a_1 exhibits a clear maximum with same location than the minimum of $-\partial J_{Na}^{(a)}/\partial n_{Na}$. This minimum stems itself from the sigmoidal activation of the pump by internal Na^+ (Eq. 9a), as negative charges shift the resting state coordinates toward the right on the activation curve of the pump, where both amplitude and sensitivity of $J_{Na}^{(a)}$ to $[Na]_i$ increase. The flux sensitivity is at its maximum when membrane charge density allows it to reach the inflexion point on the activation curve of the pump, corresponding to the maximum degree of stability.

The above mechanism is almost insensitive to the magnitude of P_{Cl}, as λ_1 depends on this membrane parameter to only an insignificant extent. However, λ_2 showed a marked dependence on P_{Cl}. With 100 times the reference value of P_{Cl}, this eigenvalue became more negative with negative charges on the membrane (not illustrated). It can be concluded that, in this case, the overall degree of stability of the cell is increased.

Influence of outer membrane charges

When the γ value decreases, the minimum of the λ_1 versus θ curve (or maximum stability) is observed for lower values of θ (Fig. 4). This shows that external charges can actually modulate the sensitivity changes of the pump to $[Na]_i$ caused by charges on the inner membrane side. In simulations where Q_o was selectively varied we could elucidate the origin of this modulation. Fig. 7 illustrates the modifications of the resting point properties when the external Ca^{2+} concentration was continuously varied from 0 to 20 mM. By increasing $[Ca]_o$ the amount of charges Q_o on the outer membrane side is reduced because part of these charges are recombining with the divalent cation (Ca^{2+} also provides a stronger charge screening than monovalent cations). Fig. 7 *A* shows that the degree of activation of the sodium pump rapidly dropped with $[Ca]_o$, as $J_{Na}^{(a)}$ diminished by >50% by going from $[Ca]_o = 0$ to $[Ca]_o = 20$ mM. To understand this effect we proceeded, as in the previous

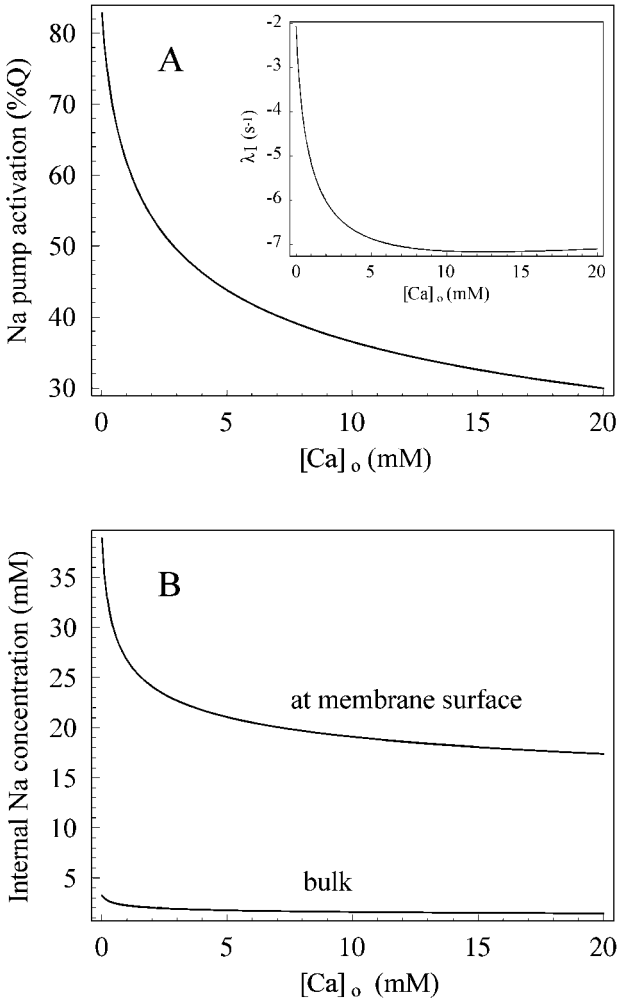

FIGURE 7 Effects of external calcium concentration, $[Ca]_o$, on internal Na^+ level and degree of activation of the sodium pump in the resting state. (A) Active Na^+ flux expressed as percent of the maximum sodium pump flux Q. (*Inset*: λ_1 eigenvalue of equation system 6, 7). (*B*) Internal Na^+ concentration in the bulk of the cytoplasm, $[Na]_i$, and at the inner side of the membrane, $[Na]_{is}$. Note that increasing $[Ca]_o$ results in more negative values of λ_1, showing that the degree of stability of the resting state is increased despite the fact that the sodium pump is inhibited. Calculations were performed with $\theta = -1.5$ and $\gamma = 1$.

section, by splitting electrostatic effects occurring on the outer side of the membrane from those on the inner side (see Eq. 8). Thus, function β, which depends on the external electrostatic potential only (Eq. 9b), diminishes by 4% from $[Ca]_o = 0$ to $[Ca]_o = 20$ mM, and thus partially explains the pump inhibition; this decrease results from the reduction of the u potential, which diminishes the pump stimulation by external K^+. Paradoxically, however, the pump inhibition mostly resulted from a decrease in the α function (which depends on the inner electrostatic potential only, see Eq. 9a), despite reduced potential v kept at the same value for all Ca^{2+} concentrations. However, the lower magnitude of the electrostatic field on the outer side of the membrane also diminished the amplitude of the Na^+ influx, thereby allowing the pump to reduce $[Na]_i$ in the resting state (Fig. 7 *B*). This decrease was very moderate (3.5 to 1.75 mM for a variation of $[Ca]_o = 0$ to $[Ca]_o = 20$ mM) and would have almost no effect on the activation of the pump were it not strongly amplified by the field of membrane superficial charges (see the $[Na]_{is}$ curve in Fig. 7 *B*). It is this amplification which allows a comparatively moderate change in bulk ionic composition to have prominent effects on $J_{Na}^{(a)}$. Finally, the inset in (Fig. 7 *A*) shows that the λ_1 eigenvalue becomes more negative when $[Ca]_o$ increases, despite the marked inhibition of the sodium pump. This confirms that heightened stability of the resting state cannot simply be explained by an acceleration of the sodium pump, but by subtle changes in the pump sensitivity to its activator cations.

DISCUSSION AND CONCLUSION

This paper presents a theoretical investigation of the influence of electrostatic fields that arise at the cell membrane surface on the basic mechanism of electro-osmotic regulation common to virtually any animal cell. Based on the experimental results of Ahrens (1981, 1983), we have introduced in our model the electrostatic control of the Na/K-ATPase into the mechanism of ion pump-leak (Hoffman and Simonsen, 1989). Ahrens (1981, 1983) showed that increasing ionic strength diminishes the Na/K-ATPase activity of bovine brain aggregates by destabilizing the formation of complexes between the ATPase and alkali metal ion activators of the enzyme. This modification of apparent binding constants was explained in a quantitative manner by the modifications of cation activities at binding sites predicted by the Gouy-Chapman theory for negative superficial charge densities (Ahrens, 1983). Similar modifications have been obtained with other enzymes anchored to the plasma membrane (including other ATPases, see Gibrat et al., 1985, and Wojtczack and Naleçz, 1985) and to the mitochondrial membrane (Krämer, 1983). Our model proposes that negative charges found at the surface of most, if not all, cells must considerably increase the speed at which ion concentrations within cells recover their resting value following the disturbances that result from the activation of physiological processes. We can therefore refer to an increase in the stability of the resting cellular state due to the presence of these charges.

This heightened stability relies more on an enhanced sensitivity of the sodium pump to increased internal bulk Na^+ concentration than on an increased resting flux of the pump, caused by the attraction of Na^+ ions to the internal side of the membrane. This mechanism requires the Na^+ bulk concentration at rest to be low enough for the pump not to be fully activated. Thomas (1972) was indeed able to stimulate the pump in snail neurons with NaCl injections, while Sokolove and Cooke (1971) showed that activation of the sodium pump due to an increase in internal Na^+ concentration is responsible for the slow adaptation in the

discharge frequency of the crayfish stretch receptor in response to sustained stimulation. Similar phenomena have been described with mammalian cells such as the dopaminergic neurons from the mesencephalon, which discharge brief bursts of action potentials interrupted by pauses, in response to NMDA applications (Johnson et al., 1992). This glutamate agonist depolarizes the membrane by letting Na^+ ions enter the cell. It is the activation of the pump by increased internal Na^+ that induces pauses in the discharge by hyperpolarizing the membrane. It is also worth mentioning the study of Thompson and Prince (1986), which shows that activation by glutamate of AMPA receptors on CA1 neurons from the hippocampus is responsible for Na^+ entry, which activates the pump of these neurons. However, Fig. 7 shows that the screening/binding of external surface charges by divalent cations increases the model stability, despite the fact that these cations inhibit the pump as well. This inhibition has been described for a number of cell types (Stankovicova et al., 1995; Hagane et al., 1989; Knudsen and Johansen, 1989; Stemer and Akera, 1988) where it appears to be nonspecific (Ca^{2+} and Mn^{2+} ions exert the same effect, Hagane et al., 1989), as in the electrostatic mechanism we postulate for this inhibition.

These conclusions go along with Ahrens's (1983) hypothesis, according to which electrostatic control of the sodium pump would play a prominent role in the capacity of the pump to achieve optimum ion concentrations inside cells. Although our model only describes the membrane transport of Na^+, K^+, and Cl^- ions, it is known that the Na/K-ATPase also contributes to the regulation of the concentration of numerous other species via the gradient of electrochemical potential of Na^+ ions that this pump establishes across the membrane. Specialized membrane transporters are coupling the endergonic transport of glucose, amino acids, neurotransmitters, and calcium to an influx of Na^+ ions. The activation of these transporters is part of the definition of the perturbations considered in this paper because it tends to dissipate the Na^+ ion gradient. It follows that the mechanism of increased stability that we propose is equally suitable to provide an increase in the stability of these other chemical species.

These conclusions obviously depend on the applicability of the Gouy-Chapman-Grahame theory to biomembranes. On the one hand, we have shown that this theory provides an adequate description of the osmotic properties of the electric double layer as long as moderate charge densities like those found on biomembranes are considered. Discrepancies between the surface potentials predicted by the Gouy-Chapman theory and the TIP equations only become significant at the limit of charge densities far above the experimental estimation of this parameter for biomembranes. On the other hand, the Gouy-Chapman theory quantitatively accounts for varied electrostatic phenomena, such as the ξ potential of phospholipidic vesicles (Winiski et al., 1986; McLaughlin and Harary, 1976), the repulsion between charged bilayers (Marra, 1986), the electric potential profile as a function of distance from the charged surface of a phospholipidic bilayer (Winiski et al., 1988), or the effects of the ionic strength on the surface potential of phospholipidic monolayers (Lakhdar-Ghazal et al., 1983; McLaughlin et al., 1971). All these phenomena, however, involve the mean electric potential, whereas ion transport only occurs at discrete sites of membranes. Therefore, not the mean electric potential but the local one is relevant for ion transport across biological membranes. The charge distribution on biomembranes is highly heterogeneous, and so low charge densities measured on these membranes pose the problem of discrete charge effects. Thus, Nelson and McQuarrie (1975) showed that the local potential due to a two-dimensional lattice array of charges deviates considerably from that given by a uniform charge distribution. However, Sauvé and Ohki (1979) subsequently showed that the linearized form of the Poisson-Boltzmann equation used by Nelson and McQuarrie (1975) ignores interactions between surface charges through their ionic atmosphere and that, in fact, the macroenvironment contributes considerably to the local potential. Sauvé and Ohki (1979) concluded that the Gouy-Chapman theory leads to an underestimation of the actual charge density near structures of membrane transport (see also Brown, 1974). Nevertheless, this theory quantitatively accounts for the shifts in the activation of a large number of ion channel types, induced by varying the ionic strength (Zhou and Jones, 1996; Yao et al., 1995; Laver and Fairley-Grenot, 1994; Kwan and Kass, 1993; Hille, 1992; Ohmori and Yoshii, 1977). These studies have produced variable estimations for charge density, but in all of them this parameter has a negative value, especially on sodium and potassium channels, which strengthens the conclusions derived from our model. More realistic approaches could be followed in the future, with the development of detailed molecular models such as those recently built for the study of lipid-protein interactions (Ben-Tal et al., 1996).

The volume of the model remains practically unchanged when the charge density is varied ($V \simeq 0.109^{-4}$ μl, Fig. 6), which allows one to directly relate the effects illustrated in Figs. 4–6 to experimentally measured charge densities. Thus, the reference charge quantity on the membrane corresponds approximately to a density of -0.07 C m^{-2} (or -1 e/220 Å^2), which represents twice the maximum estimate computed from electrophoretic mobility experiments (Wojtczak and Naleçz, 1985). However, this estimate represents a mean density far smaller than the values that need to be considered to explain the effects of ionic strength on the activation curve of voltage-dependent ion channels (Hille et al., 1975; Gilbert and Ehrenstein, 1984). These latter values should in fact be compared with the model results, as they are actually relevant to the processes of membrane ion transport. For instance, Hille et al. (1975) gave an estimate of -1 e/111 Å^2 for the charge density at the entrance of the sodium channel of the toad nerve, which

is approximately twice the reference density in our model, a value that coincides with the domain where negative charges induce the maximum stability. It is noteworthy that for these values the model variables take values that correspond to those measured experimentally. Thus, the Na^+ ion concentration is on the order of a few millimolar, whereas the K^+ ion concentration is approximately a hundred millimolar. Moreover, the macroscopic potential φ_m falls between -64 and -66 mV, all of which are fairly common values for the membrane potential. The results presented here could therefore serve as a basis for future experimental studies of cell ion dynamics in response to pathophysiological disturbances by using microfluorescence methods.

APPENDIX

Algebraic equations 10, 11, 12, 13, and 15 derive from ordinary differential equations describing the time evolution of variables n_{Cl}, V, u, v, and w, and into which the approximation of quasi-stationarity was introduced (Heinrich and Schuster, 1996). Equation 11 thus arises from the equation:

$$C_m \frac{d\varphi_t}{dt} = F\left(\frac{dn_{Na}}{dt} + \frac{dn_K}{dt} - \frac{dn_{Cl}}{dt}\right), \tag{A1}$$

where C_m denotes the electric capacitance of the membrane. In the present case, the assumption of quasi-stationarity is based on the fact that, with common specific C_m values (typically 1 μF cm^{-2}, Hille (1992)), the time constant of the capacitive charge of the membrane is so short, compared to that of the evolution of internal ion mole numbers and of cell volume, that the fast process described in Eq. A1 can be considered at all time in equilibrium. By proceeding in the same manner with the differential equations of the other variables, we obtained the system of algebraic equations 10, 11, 12, 13, and 15 which, together with Eqs. 6 and 7, constitute the degenerate system of the initial differential system, which describes the dynamics of the model.

To simplify the typography, we introduce the following notation:

$$x_1 = n_{Na} \quad x_2 = n_K \tag{A2}$$

$$y_1 = n_{Cl} \quad y_2 = V \quad y_3 = u \quad y_4 = v \quad y_5 = w, \tag{A3}$$

and we define the following vectors:

$$\mathbf{X}(t) = (x_1(t), x_2(t))^\top \tag{A4}$$

$$\mathbf{Y}(t) = (y_1(t), y_2(t), y_3(t), y_4(t), y_5(t))^\top. \tag{A5}$$

This allows us to rewrite the algebro-differential system in the following form:

$$\frac{d\mathbf{X}}{dt} = \mathbf{f}(\mathbf{X},\mathbf{Y}) \tag{A6}$$

$$\mathbf{g}(\mathbf{X},\mathbf{Y}) = 0 \tag{A7}$$

where

$$\mathbf{f}(\mathbf{X},\mathbf{Y}) = (\mathbf{f}_1(\mathbf{X}, \mathbf{Y}), \mathbf{f}_2(\mathbf{X}, \mathbf{Y}))^\top \tag{A8}$$

$$\mathbf{g}(\mathbf{X}, \mathbf{Y}) = (\mathbf{g}_1(\mathbf{X}, \mathbf{Y}), \mathbf{g}_2(\mathbf{X}, \mathbf{Y}), \mathbf{g}_3(\mathbf{X}, \mathbf{Y}), \mathbf{g}_4(\mathbf{X}, \mathbf{Y}), \mathbf{g}_5(\mathbf{X}, \mathbf{Y}))^\top. \tag{A9}$$

Let $(\bar{\mathbf{X}}, \bar{\mathbf{Y}})$ denote the equilibrium point of system A6, A7. It is easily verified that an open set Ω in $\mathbb{R}_+^{*2} \times \mathbb{R}_+^{*2}$ can be found such that:

1. $(\bar{\mathbf{X}}, \bar{\mathbf{Y}})$ belongs to Ω;
2. Function $\mathbf{g}$ is of class C^1 in Ω;
3. The Jacobian matrix $\partial\mathbf{g}/\partial\mathbf{Y}(\bar{\mathbf{X}}, \bar{\mathbf{Y}})$ is non-singular.

Recalling that $\mathbf{g}(\bar{\mathbf{X}}, \bar{\mathbf{Y}}) = 0$, we can apply the implicit function theorem (see Zeidler (1995), pp. 250 ff.) which guarantees that:

1. In a neighborhood of $(\bar{\mathbf{X}}, \bar{\mathbf{Y}})$, $\mathbf{Y}$ can be expressed as a C^1 function of $\mathbf{X}$, that is:

$$\mathbf{Y} = \mathbf{h}(\mathbf{X}), \tag{A10}$$

2. The Jacobian matrix $\partial\mathbf{h}/\partial\mathbf{X}$ can be written as:

$$\frac{\partial\mathbf{h}}{\partial\mathbf{X}} = -\left(\frac{\partial\mathbf{g}}{\partial\mathbf{Y}}\right)^{-1}\frac{\partial\mathbf{g}}{\partial\mathbf{X}}. \tag{A11}$$

We can therefore rewrite system (A6, A7) as:

$$\frac{d\mathbf{X}}{dt} = \mathbf{F}(\mathbf{X}, \mathbf{h}(\mathbf{X})), \tag{A12}$$

or, more simply:

$$\frac{d\mathbf{X}}{dt} = \bar{\mathbf{F}}(\mathbf{X}). \tag{A13}$$

This reduction of dimensionality in the initial system allows the study of a system in $\mathbb{R}^2$. Stability of the stationary point $(\bar{\mathbf{X}}, \bar{\mathbf{Y}})$ was studied by considering the behavior of a vector of small perturbations $\delta\mathbf{X}(t) = \mathbf{X}(t) - \bar{\mathbf{X}}$ verifying

$$\frac{d\delta\mathbf{X}}{dt} = \mathbf{J}\delta\mathbf{X}, \tag{A14}$$

in which $\mathbf{J}$ is the Jacobian matrix of system (A13):

$$\mathbf{J} = \frac{\partial\bar{\mathbf{F}}}{\partial\mathbf{X}}(\bar{\mathbf{X}}) = \begin{pmatrix} \frac{\partial\bar{F}_1}{\partial x_1}(\bar{\mathbf{X}}) & \frac{\partial\bar{F}_1}{\partial x_2}(\bar{\mathbf{X}}) \\ \frac{\partial\bar{F}_2}{\partial x_1}(\bar{\mathbf{X}}) & \frac{\partial\bar{F}_2}{\partial x_2}(\bar{\mathbf{X}}) \end{pmatrix}. \tag{A15}$$

Coefficients of $\mathbf{J}$ are obtained with the chain rule of differentiation (see, for example, Courant (1936), pp. 71 ff.):

$$\begin{aligned}
\frac{\partial\bar{F}_1}{\partial n_{Na}} &= \frac{\partial f_1}{\partial n_{Na}} + \sum_{i=1}^{5}\frac{\partial f_1}{\partial y_i}\frac{\partial y_i}{\partial n_{Na}} = \frac{\partial f_1}{\partial n_{Na}} + \sum_{i=1}^{5}\frac{\partial f_1}{\partial y_i}\frac{\partial h_i}{\partial n_{Na}} \\
\frac{\partial\bar{F}_1}{\partial n_K} &= \frac{\partial f_1}{\partial n_K} + \sum_{i=1}^{5}\frac{\partial f_1}{\partial y_i}\frac{\partial y_i}{\partial n_K} = \frac{\partial f_1}{\partial n_K} + \sum_{i=1}^{5}\frac{\partial f_1}{\partial y_i}\frac{\partial h_i}{\partial n_K} \\
\frac{\partial\bar{F}_2}{\partial n_{Na}} &= \frac{\partial f_2}{\partial n_{Na}} + \sum_{i=1}^{5}\frac{\partial f_2}{\partial y_i}\frac{\partial y_i}{\partial n_{Na}} = \frac{\partial f_2}{\partial n_{Na}} + \sum_{i=1}^{5}\frac{\partial f_2}{\partial y_i}\frac{\partial h_i}{\partial n_{Na}} \\
\frac{\partial\bar{F}_2}{\partial n_K} &= \frac{\partial f_2}{\partial n_K} + \sum_{i=1}^{5}\frac{\partial f_2}{\partial y_i}\frac{\partial y_i}{\partial n_K} = \frac{\partial f_2}{\partial n_K} + \sum_{i=1}^{5}\frac{\partial f_2}{\partial y_i}\frac{\partial h_i}{\partial n_K},
\end{aligned} \tag{A16}$$

the matrix elements $\partial h_i/\partial x_1$ and $\partial h_i/\partial x_2$, $i = 1, \ldots, 5$ in (A16) being the coefficients of the Jacobian matrix $\partial \mathbf{h}/\partial \mathbf{X}$, which appears in Eq. A11. Solutions of the linearized system can be written as:

$$\delta \mathbf{X}(t) = \sum_{i=1}^{2} \mathbf{C}_i \exp(\lambda_i t), \qquad \text{(A17)}$$

where the $\mathbf{C}_i$ are column vectors in $\mathbb{R}^2$, whose components are set by initial conditions and where the λ_i are the eigenvalues of $\mathbf{J}$. If the real part of the eigenvalues, computed at the stationary point, are strictly negative, then this point is asymptotically stable. Equation A17 also recalls that it is necessary and sufficient for the real part of the two eigenvalues to be strictly inferior to $-\alpha$, $\alpha \in \mathbb{R}_+$ for the point to be stable with degree α (Bourlès, 1986).

The authors thank Profs. J.-P. Badiali (Université Pierre et Marie Curie, Paris, France), Y. Bouligand (Université d'Angers, France), and C. Ripoll (Université de Rouen, France) for fruitful discussions, and Dr. Mark Mayer (Université Pierre et Marie Curie, France) for correcting the English.

REFERENCES

Ahrens, M.-L. 1981. Electrostatic control by lipids upon the membrane-bound (Na^+-K^+)-ATPase. *Biochim. Biophys. Acta.* 642:1–10.

Ahrens, M.-L. 1983. Electrostatic control by lipids upon the membrane-bound (Na^+-K^+)-ATPase. II. The influence of surface potential upon the activating ion equilibria. *Biochim. Biophys. Acta.* 732:252–266.

Apell, H.-J. 1989. Electrogenic properties of the Na, K pump. *J. Membr. Biol.* 110:103–114.

Ben-Tal, N., B. Honig, R. M. Peitzsch, G. Denisov, and S. McLaughlin. 1996. Binding of small basic peptides to membranes containing acidic lipids: theoretical models and experimental results. *Biophys. J.* 71: 561–575.

Bourlès, H. 1986. Stabilité de degré α des systèmes régis par une équation différentielle fonctionnelle. *RAIRO APII.* 19:455–473.

Brown, R. H., Jr. 1974. Membrane surface charge: discrete and uniform modelling. *Prog. Biophys. Mol. Biol.* 28:341–370.

Cevc, G. 1990. Membrane electrostatics. *Biochim. Biophys. Acta.* 1031: 311–382.

Courant, R. 1988. Differential and Integral Calculus, Vol. II Wiley, New York, 1936; Wiley Classics Library Edition Published 1988.

De Groot, S. R., and P. Mazur. 1984. Non-Equilibrium Thermodynamics. Dover Publications, Inc., New York.

Durand-Vidal, S., J.-P. Simonin, and P. Turq. 2000. Electrolytes at Interfaces. Kluwer Academic Press, Dordrecht, The Netherlands.

Eyges, L. 1980. The Classical Electromagnetic Field. Dover Publications, Inc., New York.

Forsten, K. E., R. E. Kozack, D. A. Lauffenburger, and S. Subramaniam. 1994. Numerical solution of the nonlinear Poisson-Boltzmann equation for a membrane-electrolyte system. *J. Phys. Chem.* 98:5580–5586.

Garay, R. P., and P. J. Garrahan. 1973. The interaction of sodium and potassium with the sodium pump in red cells. *J. Physiol. (Lond.).* 213:297–325.

Genet, S., and J. Cohen. 1996. The cation distribution set by surface charges explains a paradoxical membrane excitability behavior. *C. R. Acad. Sci. Paris.* 319:263–268.

Genet, S., R. Costalat, and J. Burger. 2000. A few comments on electrostatic interactions in cell physiology. *Acta. Biotheor.* 48:273–287.

Gibrat, R., J.-P. Grouzis, J. Rigaud, and C. Grignon. 1985. Electrostatic characteristics of corn root plasmalemma: effect on the Mg^{2+}-ATPase activity. *Biochim. Biophys. Acta.* 816:349–357.

Gilbert, D. L., and G. Ehrenstein. 1984. Membrane surface charge. *Curr. Topics Membr. Transp.* 22:407–421.

Goldman, D. 1943. Potential, impedance, and rectification in membranes. *J. Gen. Physiol.* 27:37–60.

Grahame, D. C. 1947. The electrical double layer and the theory of electrocapillarity. *Chem. Rev.* 41:441–501.

Hagane, K., T. Akera, and P. Stemmer. 1989. Effects of Ca^{2+} on the sodium pump observed in cardiac myocytes isolated from guinea pigs. *Biochim. Biophys. Acta.* 982:279–287.

Heinrich, R., and S. Schuster. 1996. The Regulation of Cellular Systems. Chapman & Hall, New York.

Hille, B. 1992. Ionic Channels of Excitable Membranes. Sinauer Press, Sunderland, MA.

Hille, B., A. N. Woodhull, and B. I. Shapiro. 1975. Negative surface charge near sodium channels of nerve: divalent ions, monovalent ions, and pH. *Phil. Trans. R. Soc. Lond. B.* 270:301–318.

Hoffman, E. K., and L. O. Simonsen. 1989. Membrane mechanisms in volume and pH regulation in vertebrate cells. *Physiol. Rev.* 69:315–382.

Jakobsson, E. 1980. Interactions of cell volume, membrane potential, and membrane transport parameters. *Am. J. Physiol. Cell Physiol.* 238: C196–C206.

Jewell, E. A., and J. B. Lingrel. 1991. Comparison of the substrate dependence properties of the rat NaK-ATPase α_1, α_2 and α_3 isoforms expressed in HeLa cells. *J. Biol. Chem.* 266:16925–16930.

Johnson, S. W., V. Seutin, and R. A. North. 1992. Burst firing in dopamine neurons induced by *N*-methyl-D-aspartate: role of electrogenic sodium pump. *Science.* 258:665–667.

Kabakov, A. 1994. The resting potential equations incorporating ionic pumps and osmotic concentration. *J. Theor. Biol.* 169:51–64.

Knudsen, T., and T. Johansen. 1989. The mode of inhibition of the Na^+-K^+ pump activity in mast cells by calcium. *Br. J. Pharmacol.* 98:1119–1126.

Krämer, R. 1983. Interaction of membrane surface charges with the reconstituted ADP/ATP-carrier from mitochondria. *Biochim. Biophys. Acta.* 735:145–159.

Kwan, Y. W., and R. S. Kass. 1993. Interactions between H^+ and Ca^{2+} near cardiac L-type calcium channels: evidence for independent channel-associated binding sites. *Biophys. J.* 65:1188–1195.

Lakhdar-Ghazal, F., J.-L. Tichadou, and J.-F. Tocanne. 1983. Effect of pH and monovalent cations on the ionization state of phosphatidylglycerol in monolayers. *Eur. J. Biochem.* 134:531–537.

Laüger, P. 1991. Electrogenic Ion Pumps. Sinauer Press, Sunderland, MA.

Laüger, P., W. Lesslauer, E. Marti, and H. Richter. 1967. Electrical properties of bimolecular phospholipid membranes. *Biochim. Biophys. Acta.* 135:20–32.

Laver, D. R., and K. A. Fairley-Grenot. 1994. Surface potential near the mouth of the large conductance K^+ channel from *Chara australis*: a method of testing for diffusion limited ion flow. *J. Membr. Biol.* 139: 149–165.

Marra, J. 1986. Direct measurement of the interaction between phosphatidylglycerol bilayers in aqueous solutions. *Biophys. J.* 50:815–825.

McLaughlin, S. 1989. The electrostatic properties of membranes. *Annu. Rev. Biophys. Chem.* 18:113–136.

McLaughlin, S., and H. Harary. 1976. The hydrophobic adsorption of charged molecules to bilayer membranes: a test of the applicability of the Stern equation. *Biochemistry.* 15:1941–1948.

McLaughlin, S. G. A., G. Szabo, and G. Eisenman. 1971. Divalent ions and the surface potential of charged phospholipid membranes. *J. Gen. Physiol.* 58:667–687.

Nelson, A. P., and D. A. McQuarrie. 1975. The effect of discrete charges on the electrical properties of a membrane. *J. Theor. Biol.* 55:13–27.

Nørby, J. G., and M. Essmann. 1997. The effect of ionic strength and specific anions on substrate binding and hydrolytic activities of Na, K-ATPase. *J. Gen. Physiol.* 109:555–570.

Ohmori, H., and M. Yoshii. 1977. Surface potential reflected in both gating and permeation mechanisms of sodium and calcium channels of the tunicate egg cell membrane. *J. Physiol. (Lond.).* 207:429–463.

Peitzsch, R. M., M. Eisenberg, K. A. Sharp, and S. McLaughlin. 1995. Calculations of the electrostatic potential adjacent to model phospholipid bilayers. *Biophys. J.* 68:729–738.

Rakowski, R. F., L. A. Vasilets, J. Latona, and W. Schwartz. 1991. A negative slope in the current-voltage relationship of the Na/K pump in *Xenopus* oocytes produced by reduction of external K. *J. Membr. Biol.* 121:177–187.

Roux, B. 1997. Influence of the membrane potential on the free energy of an intrinsic protein. *Biophys. J.* 73:2980–2989.

Sanfeld, A. 1968. Introduction to the Thermodynamic of Charged and Polarized Layers. Monographs in Statistical Physics, Vol. 10. John Wiley & Sons, Ltd., New York.

Sauvé, R., and S. Ohki. 1979. Interactions of divalent cations with negatively charged membrane surfaces. I. Discrete charge potential. *J. Theor. Biol.* 81:157–179.

Sharp, K. A., and B. Honig. 1990. Electrostatic interactions in macromolecules: theory and applications. *Annu. Rev. Biophys. Chem.* 19:301–332.

Sokolove, P. G., and I. M. Cooke. 1971. Inhibition of impulse activity in a sensory neuron by an electrogenic sodium pump. *J. Gen. Physiol.* 57:125–163.

Stafiej, J., Z. Ekoba, Z. Borkowska, and J. P. Badiali. 1996. New theoretical description of electrified interfaces. *J. Chem. Soc., Faraday Trans.* 92:3677–3682.

Stankovicova, T., H. Zemkova, A. Breier, E. Amler, M. Burkhard, and F. Vyskocil. 1995. The effects of calcium and calcium channel blockers on sodium pump. *Pflügers Arch. Eur. J. Physiol.* 429:716–721.

Stemer, P., and T. Akera. 1988. Sodium-pump activity and its inhibition by extracellular calcium in cardiac myocytes of guinea pigs. *Biochim. Biophys. Acta.* 940:188–196.

Thomas, R. C. 1972. Intracellular sodium activity and the sodium pump in snail neurons. *J. Physiol. (Lond.).* 220:55–71.

Thompson, S. M., and D. A. Prince. 1986. Activation of electrogenic sodium pump in hippocampal CA1 neurons following glutamate-induced depolarization. *J. Neurophysiol.* 56:507–522.

Vasilets, L. A., T. Ohta, S. Nogushi, M. Kawamura, and W. Schwartz. 1993. Voltage dependent inhibition of the sodium pump by external sodium: species differences and possible role of the N-terminus of the α-subunit. *Eur. Biophys. J.* 21:433–443.

Winiski, A. P., M. Eisenberg, M. Langner, and S. McLaughlin. 1988. Flurorescent probes of electrostatic potential 1 nm from the membrane surface. *Biochemistry.* 27:386–392.

Winiski, A. P., A. C. McLaughlin, R. V. McDaniel, M. Eisenberg, and S. McLaughlin. 1986. An experimental test of the discreteness-of-charge effect in positive and negative bilayers. *Biochemistry.* 25:8206–8214.

Winterhalter, M., and W. Helfrich. 1988. Effect of surface charge on the curvature elasticity of membranes. *J. Phys. Chem.* 92:6865–6867.

Wojtczak, L., and M. J. Naleçz. 1985. The surface potential of membranes: its effect on membrane-bound enzymes and transport processes. *In* Structure Properties of Cell Membranes, Vol. 2. G. Benga, editor. CRC Press, Boca Raton, FL. 215–242.

Yao, J-A., N. C. Saxena, M. R. Ziai, S. Ling, and G-N. Tseng. 1995. Effects of *n*-Dodecylguanidine on A-type potassium channels: role of external surface charges in channel gating. *Mol. Pharmacol.* 48: 160–171.

Zeidler, E. 1995. Applied Functional Analysis. Main Principles and Their Applications. Springer-Verlag, New York-Berlin-Heidelberg.

Zhou, W., and W. Jones. 1996. The effects of external pH on calcium channel currents in bullfrog sympathetic neurons. *Biophys. J.* 70: 1326–1334.